Rectangular nanovoids in helium-implanted and thermally annealed MgO(100)

Kooi, B. J.; van Veen, A. ; de Hosson, J. Th. M. ; Schut, H.; Fedorov, A. V.; Labohm, F.

Published in:
Applied Physics Letters

DOI:
10.1063/1.125954

Publication date:
2000

Rectangular nanovoids in helium-implanted and thermally annealed MgO(100)

B. J. Kooi, A. van Veen, and J. Th. M. De Hosson[a)]
Department of Applied Physics, Materials Science Center and the Netherlands Institute for Metals Research, University of Groningen, Nijenborgh 4, 4797AG Groningen, The Netherlands

H. Schut, A. V. Fedorov, and F. Labohm
Interfaculty Reactor Institute, Delft University of Technology, Mekelweg 15, 2629JB Delft, The Netherlands

(Received 9 November 1999; accepted for publication 5 January 2000)

Cleaved MgO(100) single crystals were implanted with 30 keV ^{3}He ions with doses varying from 1×10^{19} to $1\times10^{20}\,m^{-2}$ and subsequently thermally annealed from 100 to 1100 °C. Transmission electron microscopy observations revealed the existence of sharply rectangular nanosize voids at a depth slightly shallower than the helium-implantation range. Monitoring of the defect depth profile and the retained amount of helium was performed by positron-beam analysis and neutron depth profiling, respectively. © *2000 American Institute of Physics.* [S0003-6951(00)01709-5]

Helium implantation followed by thermal annealing at elevated temperature leads, in a number of semiconductor and ceramic materials, to void generation. First, it was demonstrated for helium-implanted silicon,[1,2] and recently for helium-and deuterium-implanted MgO.[3,4] In this letter, we will show by transmission electron microscopy (TEM) that the cavities have adopted a very special rectangular morphology. The presented results hold the promise that nanocavities can be produced at a desired depth and with a desired size.

Samples obtained by cleaving of MgO(100) crystals to a thickness of 1 mm and a size of $1\times1\,cm^2$ were implanted with a dose varying from 1×10^{19} to $1\times10^{20}\,m^{-2}$ ^{3}He ions with 30 keV energy. Thermal annealing of the samples was performed in a longitudinal oven in ambient air during 30 min. After each annealing step, the samples were analyzed by photon absorption and positron-beam analysis. Photon absorption revealed the presence of *F* centers in the as-implanted sample, which disappeared after annealing to 500 K. For the high-dose-implanted samples annealed at 1370 K, positron-beam analysis indicated the presence of voids with nanometer size at a depth somewhat shallower than that of the helium-implantation depth.[3] In a similar experiment, it was shown using neutron depth profiling that helium is released from the cavities at a temperature of about 1300 K.[3]

For cross-sectional TEM examination, slices with a thickness of about 1 mm were obtained from the MgO single crystal with the voids using cleavage fracture along {100}. Two slices were glued together with the original surfaces exposed to implantation facing each other and separated by the glue (Gatan G-1 epoxy and hardener). The coupled slices of MgO were glued in cross-section geometry on a Cu ring (3 mm outer and 2 mm inner diameter). Then, the MgO was ground and polished to a thickness of about 100 μm. Using dimpling from the Cu side, the thickness of the MgO in the center of the ring is reduced to about 25 μm. Finally, the dimpled sample was thinned to electron transparency by two beams of 4 kV Ar^+ ions making an angle of 6° with the top and bottom sample surfaces using a Gatan PIPS 691. TEM observations were performed using a JEOL 4000 EX/II operating at 400 kV (point-to-point resolution 0.165 nm).

An overview of the implanted top layer of the MgO is shown in the bright-field TEM image of Fig. 1 (viewing direction close to [001] and in a two-beam condition with the other strong beam $g=220$). At a distance of about 50–60 nm from the edge of the foil a localized band of rectangular features can be observed. These rectangular features are visible due to Fresnel contrast resulting in a bright outer fringe and a dark inner fringe, indicating the overfocus condition during imaging. Figure 2 shows the rectangular features in underfocus condition. The Fresnel contrast makes clear that rectangularly shaped voids due to the He implantation and the annealing are present in the MgO with observable sizes of the edges ranging between 0 and 20 nm. The crystal orientation of the MgO is well defined (with the edge of the TEM specimen still more or less parallel to the original implanted surface) and the sides of the rectangular voids correspond to cube planes of the MgO. The present results clearly

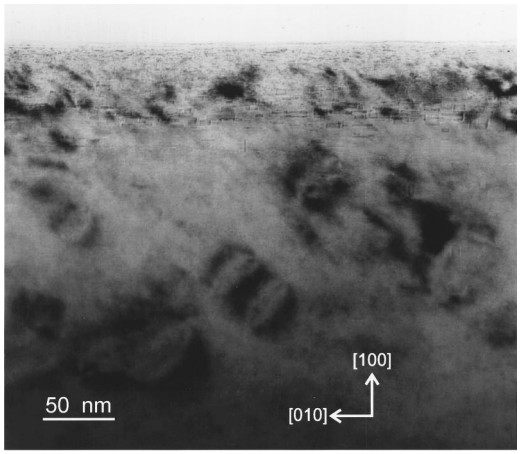

FIG. 1. Bright-field TEM image (two-beam condition with the other strong beam $g=220$) showing an overview of the implanted top layer revealing the presence of sharply rectangular nanocavities as seen by Fresnel contrast in overfocused condition.

[a)]Author to whom correspondence should be addressed; electronic mail: hossonj@phys.rug.nl

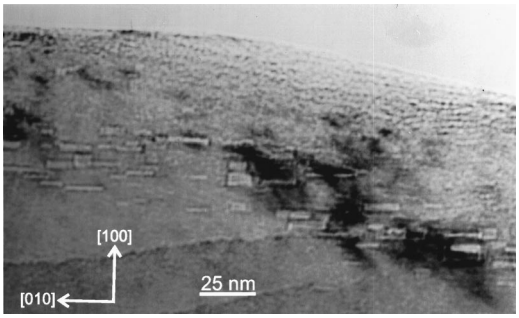

FIG. 2. Bright-field TEM image (two-beam condition with viewing direction near [001] and with the other strong beam $g=220$) showing sharply rectangular nanocavities as seen by Fresnel contrast in underfocused condition.

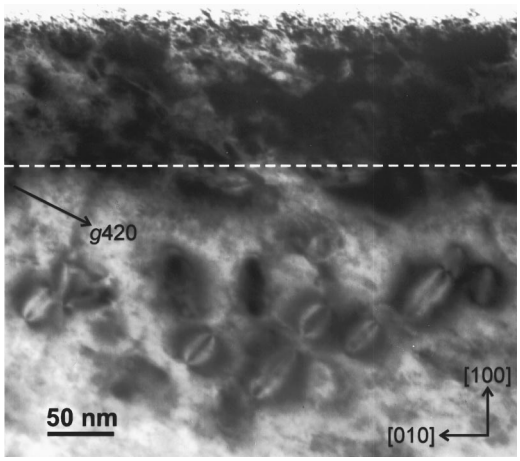

FIG. 3. Strong-beam dark-field TEM image for a viewing direction near [001] with $g=420$ showing dislocation loop contrast at a depth in between 150 and 300 nm. The white dashed line at a depth of 120 nm indicates the center of the region where the rectangular voids are present (they are not visible in the present micrograph but are clearly traceable in the original negative). For reasons of clarity the intensity scale of the image is inverted, i.e., the gray scale from black to white is white to black instead.

indicate that already for voids in the nanometer scale range in MgO a very strong tendency for faceting is present. This is uncommon for nanoscale voids (bubbles) obtained after He implantation and annealing in metals[5] or semiconductors[1] and previously investigated ceramics such as α-Al_2O_3.[6–10] Then, the nanovoids are spherical and only for increased sizes (e.g., larger than a few tens of nm) they become facetted.[2,6,7]

The origin of the strong tendency for faceting in the MgO system is most probably related to the high (Pauling's) ionicity of MgO. The surface energy for different facets of MgO is largely determined by the polarity of the terminating plane. Nonpolar surfaces have finite energies, whereas in the case of a dipole moment in the repeat unit perpendicular to the surface, the energy diverges and becomes infinite.[11] Hence, for highly ionic systems spherical voids are, even at a size of a nanometer, unfavorable, because locally an uncompensated dipole moment perpendicular to the surface may result.

The shape of the voids is expected to be independent of its size when the Wulff construction is applied. However, for decreasing size of the cavities the fraction of atoms on or near edges and also of atoms in or close to corners that contribute to the total energy of the cavity increases. Hence, the prediction of the shape by the surface energy of individual facets alone will no longer apply. Minimization of the surface area with respect to the enclosed volume tends to have a controlling influence on the shape of the void. For metals and semiconductors and ceramics aforementioned this mechanism, which leads to small spherical cavities, applies but for voids in MgO it does not. Apparently, due to the extreme anisotropy in energy of atoms in different surface states, the voids in MgO are bounded by cube planes of the MgO, independent of the size of the cavities. In literature, surface energies for MgO(111) and (110) are quoted to be a factor 2–4 times larger than for the (100) surface.[12]

In the region within 50–60 nm from the edge in Fig. 1 hardly any cavities are found, indicating the locally low-He concentration after implantation. Helium in this region can have formed undetectably small clusters or can have diffused to earlier nucleated cavities at larger depth or to the surface followed by desorption. At a larger distance from the edge than where the cavities are located, other sharply contrasting features can be observed in Fig. 1. These features become more apparent at a distance of about 250 nm from the edge in Fig. 3, showing a strong-beam dark-field image for viewing near [001] for $g=420$, as indicated by the arrow. Note that the dark-field image is inverted for reasons of clarity, i.e., the gray scale from black to white is white to black instead. These features can be identified as dislocation loops, often with the same inclination to the viewing direction. Dislocation loop contrast may also originate from (partially) coherent precipitates.[13] However, in the present context of He implantation and annealing the presence of dislocation loops is not surprising, whereas of precipitates it is unlikely. Dislocation loops in MgO as a result of irradiation damage followed by annealing were found to be of interstitial type with a Burgers vector of $\frac{1}{2}\langle 110\rangle$.[6] The low density and large sizes of the dislocation loops compared to the cavities indicate the low concentration of implanted He and large diffusion distances at the depth of the dislocation loops.

The white dashed line in Fig. 3 indicates the center of the region where the cavities are localized; although not visible in Fig. 3, they could be well recognized on the original negative. For determination of the depth of the cavities and the dislocation loops below the original sample surface Fig. 1 is not suitable, because during preparation of the TEM sample a part of the top layer has been removed by ion milling. On the other hand, Fig. 3 is suitable for obtaining the depth of the voids and dislocation loops since the region imaged in Fig. 3 is very close to unremoved glue between the surfaces of the two MgO slices. Therefore, we can be sure that the cavities are located at a depth of about 120 nm (almost all localized in between 100–140 nm) and the dislocation loops are localized at a depth of 150–350 nm (mostly at a depth of about 250 nm).

As mentioned earlier, positron-beam analysis had been performed on the sample before TEM examination. Positrons have a high affinity for trapping at vacancies and agglomerates of vacancies or voids. In general, the 511 keV photon peak observed due to annihilation of the positron with an electron from the sample is Doppler broadened. The electron carries a certain momentum component to or from the detec-

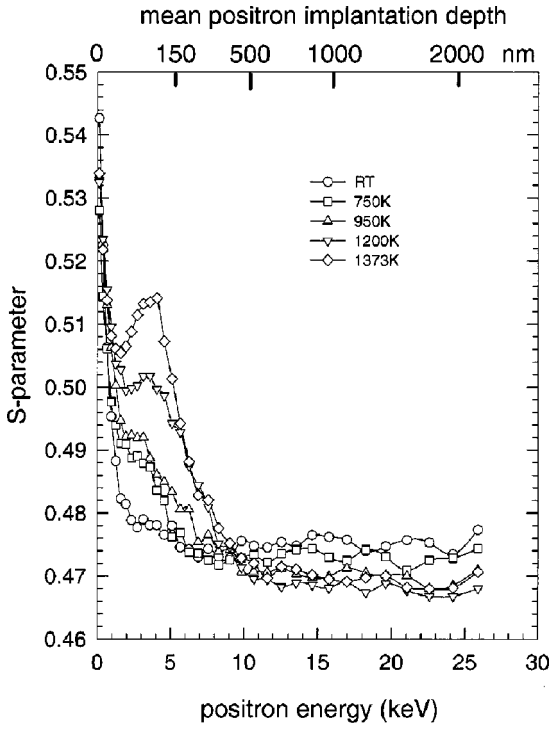

FIG. 4. The *S* parameter as a function of positron energy for the $1\times10^{16}\,\mathrm{cm}^{-2}$ ^{3}He-implanted MgO(100) crystal after annealing at the indicated temperatures. The mean probe depth of the positrons is indicated in the top scale. Note the increase of the *S* parameter upon annealing at the depth corresponding with the cavity layer from Fig. 3.

tor so that broadening occurs. The momentum of the electrons encountered in the defects is generally lower than in the bulk and, therefore, broadening is reduced in that case. When the cavity is larger than about 0.8 nm positronium, i.e., the bound e^+-e^- pair, is formed in the cavity which annihilates with even less broadening. The shape of the peak is characterized quantitatively with the aid of two parameters *S* and *W*. *S* accounts for the weight of the low-momentum contributions and *W* for the high-momentum contributions. In this letter, we will use the *S*-parameter versus positron-implantation-energy measurements to investigate the depth profile of the formed cavities.

The positron results are shown in Fig. 4, where the *S* vs *E* curves obtained for several annealing temperatures are plotted. By fitting the results with a three-layer model allowing for diffusion and defect trapping of the positrons, two defect layers are identified on the substrate.[4] The first layer is the layer where, according to TRIM calculations,[14] displacement damage without helium is produced by the helium implantation. During annealing, the *S* parameter increases gradually from a value of 0.478 to a saturation value of 0.505 at 1200 K. This indicates that some vacancy clustering occurred in the layer. In the second layer, where the helium was implanted and displacement damage reached its maximum the bubbles were formed, which after helium release turned into the observed cavities. The fitted *S*-parameter 0.523 found for that layer clearly indicates the formation of positronium in line with the microscopic observation. The zone of depth where the cavities are found coincides rather well with defect layer 2. The best fit was obtained for a zone from 100 to 140 nm. For the sample with half the helium-implantation dose of the TEM sample, the annealing was continued to higher temperature. It was observed that the cavities disappeared at 1500 K. At that temperature, self-diffusion is a sufficiently fast process to let shrinkage of the cavities occur. We explain the formation of the cavities by the stabilization of helium during the early stages of vacancy clustering. Helium prevents the vacancy clusters to collapse to dislocation loops, therefore, three-dimensional clusters are formed. The growth of the helium-filled vacancy clusters proceeds by an Ostwald ripening process. The final stage is the release of helium from the bubbles by permeation through the top layer of the material.

It appears that a temperature window exists from 1200 to 1400 K in which helium is permeating while the cavities remain thermally stable. In an earlier work[8] where MgO was neutron irradiated, cavities or voids were never observed. Apparently, it is essential to have a sufficiently high gas concentration in MgO to promote void formation. It is well known that for a variety of ceramic materials, e.g., Al_2O_3 exposed to neutron irradiation, ordered void structures are developed.[6] It is likely that gases, notably transmutation-produced helium, are involved which may stabilize the growing voids. In contrast to metals, where helium remains bound and stabilizes the cavities or bubbles to temperatures close to melting, in the above ceramics helium permeates from the cavities to the vacuum at much lower temperature and leaves cavities behind which are stable to temperatures where they dissolve by vacancy dissociation. If the implanted atom has a higher solubility than helium or hydrogen, nanoprecipitates in the case of metal atoms or gas bubbles in the case of the heavier noble gas atoms are observed.[15–17]

The present work has shown that rectangular and flat nanosize cavities are formed which have a thickness generally much smaller than the lateral dimensions. The cavities form an interesting materials-testing laboratory in a nanoworld protected from the environment.

[1] C. C. Griffioen, J. H. Evans, P. C. de Jong, and A. van Veen, Nucl. Instrum. Methods Phys. Res. B **27**, 417 (1987).
[2] S. M. Myers, D. M. Bishop, D. M. Follstaedt, H. J. Stein, and W. R. Wampler, Mater. Res. Soc. Symp. Proc. **238**, 549 (1996).
[3] H. Schut, A. van Veen, F. Labohm, A. V. Fedorov, E. A. C. Neeft, and R. J. M. Konings, Nucl. Instrum. Methods Phys. Res. B **147**, 212 (1999).
[4] A. van Veen, H. Schut, A. V. Fedorov, F. Labohm, E. A. C. Neeft, and R. J. M. Konings, Nucl. Instrum. Methods Phys. Res. B **148**, 768 (1999).
[5] J. H. Evans and D. J. Mazey, J. Phys. **15**, L1 (1985).
[6] F. W. Clinard, G. F. Hurley, and L. W. Hobbs, J. Nucl. Mater. **108-109**, 655 (1982).
[7] F. Freund, R. Knobel, H. Kathrein, and H. Wengeler, Nucl. Instrum. Methods Phys. Res. B **1**, 223 (1984).
[8] S. J. Zinkle and S. Kojima, J. Nucl. Mater. **179-181**, 395 (1991).
[9] W. E. Lee, M. L. Jenkins, and G. P. Pells, Philos. Mag. A **51**, 639 (1985).
[10] Y. Katano, H. Ohno, and H. Katsuta, J. Nucl. Mater. **155-157**, 366 (1988).
[11] P. W. Tasker, J. Phys. C **12**, 4977 (1979).
[12] G. W. Watson, E. T. Kelsey, N. H. de Leeuw, D. J. Harris, and S. C. Parker, Faraday Trans. **92**, 433 (1996).
[13] P. B. Hirsch, A. Howie, R. B. Nicholson, D. W. Pashley, and M. J. Whelan, *Electron Microscopy of Thin Crystals* (Butterworths, London, 1965).
[14] J. F. Ziegler, J. P. Biersack, and U. Littmark, *The Stopping and Range of Ions in Solids (TRIM)* (Pergamon, New York, 1985).
[15] Y. Qian, D. Ila, R. L. Zimmermann, D. B. Poker, L. A. Boatner, and D. K. Hensley, Nucl. Instrum. Methods Phys. Res. B **127**, 524 (1997).
[16] J. H. Evans, J. Nucl. Mater. **210**, 21 (1994).
[17] A. Briggs, J. Mater. Sci. **10**, 729 (1975).